Temperature dependence of the photoluminescence of MnS/ZnS core–shell quantum dots*

Fang Dai-Feng(房岱峰)[a], Ding Xing(丁 星)[b], Dai Ru-Cheng(代如成)[c]†,
Zhao Zhi(赵 智)[a], Wang Zhong-Ping(王中平)[c], and Zhang Zeng-Ming(张增明)[c]

[a] *Hefei National Laboratory for Physical Sciences at Microscale and Department of Physics, University of Science and Technology of China, Hefei* 230026, *China*
[b] *Physics Department, Anhui University, Hefei* 230601, *China*
[c] *Center of Physical Experiments, University of Science and Technology of China, Hefei* 230026, *China*

(Received 3 June 2014; revised manuscript received 7 August 2014; published online 10 October 2014)

The temperature dependence of the photoluminescence (PL) from MnS/ZnS core–shell quantum dots is investigated in a temperature range of 8 K–300 K. The orange emission from the $^4T_1 \rightarrow {}^6A_1$ transition of Mn^{2+} ions and the blue emission related to the trapped surface state are observed in the MnS/ZnS core–shell quantum dots. As the temperature increases, the orange emission is shifted toward a shorter wavelength while the blue emission is shifted towards the longer wavelength. Both the orange and blue emissions reduce their intensities with the increase of temperature but the blue emission is quenched faster. The temperature-dependent luminescence intensities of the two emissions are well explained by the thermal quenching theory.

Keywords: MnS/ZnS, quantum dots, temperature, photoluminescence

PACS: 78.67.–n, 78.55.Et, 78.67.Hc **DOI:** 10.1088/1674-1056/23/12/127804

1. Introduction

Zinc sulfide (ZnS) is an important wide band gap (E_g = 3.6 eV) semiconductor, which has been widely used in ultraviolet-light-emitting diodes, electroluminescencent devices, flat-panel displays, sensors, and injection lasers.[1–5] Transition-metal Mn^{2+} ion-doped ZnS (ZnS:Mn) attracts a great deal of attention, for Mn^{2+} doping can not only enhance its optical transition efficiency, but also induce interesting magneto–optical properties.[6–8] Nanoscale ZnS:Mn material has been the current focus of research; the synthesis method and the properties of the material have been reported. Unfortunately, because of the high surface-to-volume ratio in a nano-material, the surface states may act as luminescence quenching centers, resulting in low luminescence efficiency.[9] Hence, the passivation of the surface is a feasible and effective way to improve the luminescence properties, such as photoluminescence (PL) quantum efficiency (PLQY), luminescence lifetime, and photo stability.[10,11] Enhanced luminescence and stability have been observed in ZnS:Mn/ZnO nanocrystals,[12] ZnS:Mn/SiO_2 nanoparticles,[13] ZnS:Mn/$Zn(OH)_2$ nanoparticles,[14] ZnS:Mn/ZnS nanocrystals,[15] and $EuVO_4$/YVO_4 nanocrystals.[16] By coating ZnS:Mn nanoparticles with an inorganic shell, the surface defects can be passivated. Therefore, the PL intensity of Mn^{2+} is enhanced through an increase of the radiative transition of Mn^{2+} centers. Zheng *et al.*[17,18] recently prepared MnS/ZnS core–shell quantum dots (QDs) with Mn-emission PLQY up to 35%. They attributed the efficient luminescence of Mn^{2+} ions to the energy transfer from photoexcited ZnS shells to the Mn^{2+} ions in a diffusion layer at the interface between the MnS core and the pure ZnS layer.

It is important to understand the interaction between the dopants in order to improve the luminescence properties. Temperature dependence of the luminescence can provide useful information about the interaction between doped ions and the host crystal lattices. Temperature variation can change the inter-atomic distance, the overlap among adjacent electronic orbits as well as the crystal field surrounding the dopant. Therefore, the study of the luminescence spectrum as a function of temperature may provide an insight into the interactions between the luminescent centers or between the centers and the host lattice. In this paper, we aim to study the temperature dependence of PL in MnS/ZnS core–shell QDs.

2. Experiment

MnS/ZnS core–shell QDs were synthesized by a nucleation-doping strategy. The detailed preparation process has been reported previously.[19] The morphologies and sizes of the samples were characterized by transmission electron microscope (TEM) (JEOL 2100). The X-ray diffraction (XRD) pattern of the synthesized sample was obtained with

*Project supported by the National Natural Science Foundation of China (Grant Nos. 11304300, 21002097, 11074232, and 11274288), the National Basic Research Program of China (Grant Nos. 2011CB932801 and 2012CB933702), the Fund from the Ministry of Education of China (Grant No. 20123402110034), the Fundamental Research Funds for the Central Universities (Grant No. WK2030420002), and the Anhui Provincial Natural Science Foundation, China (Grant No. 1308085QA06).

†Corresponding author. E-mail: dairc@ustc.edu.cn

© 2014 Chinese Physical Society and IOP Publishing Ltd

an X-ray diffraction facility (TTR-III). The X-ray photoelectron spectroscopy (XPS) spectra were recorded on ESCALAB 250 with Mg K_α-line (1253.6 eV) as an X-ray excitation source. Temperature-dependent PL spectra were measured by a steady-state/lifetime spectrofluorimeter (FLUOROLOG-3-TAU, Jobin Yvon) in a temperature range of 8 K–300 K.

3. Results and discussion

Figure 1 shows the TEM image of the as-prepared MnS/ZnS core–shell QDs. It can be seen that the MnS/ZnS QDs are uniform spherical-shaped particles. The diameters of the MnS cores and the MnS/ZnS QDs are determined to be 2.3 nm and 5 nm, respectively. The thickness of the ZnS shells is thus estimated to be about 1.4 nm. Figure 2 shows the XRD spectrum of the MnS/ZnS core–shell QDs. All the diffraction peaks can be indexed to be a cubic zinc blende structure, which is consistent with the standard card (JCPDS No. 77-2100).

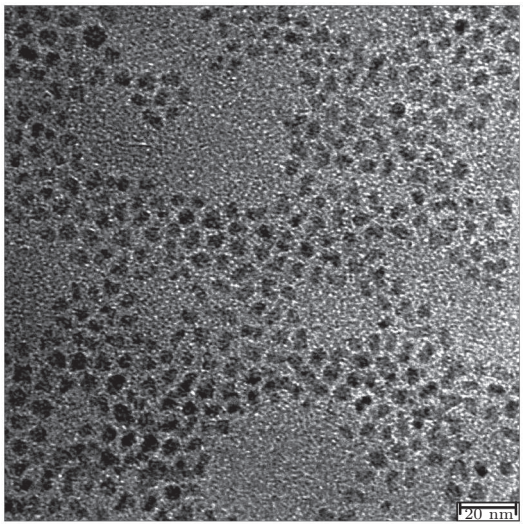


Fig. 1. TEM image of as-prepared MnS/ZnS core–shell QDs.

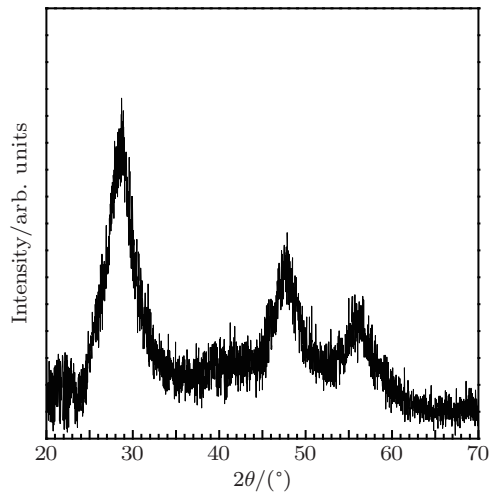


Fig. 2. X-ray diffraction pattern of MnS/ZnS core–shell QDs.

To further characterize the as-synthesized samples, we carry out an XPS measurement to investigate the surface compositions and chemical state of MnS/ZnS core–shell QDs, and the result is shown in Fig. 3. The inelastic mean free path (IMFP) is less than 1 nm for the generated Mn 2p photoelectrons with an energy of about 500 eV. IMFP for Zn 2p photoelectrons is much shorter. So the spectrum signals should be dominated by the ZnS shell. The intensity of the Zn $2p_{3/2}$ peak in MnS/ZnS core–shell QDs is much stronger than that of the Mn XPS line (at $\sim$ 640 eV, marked with a dashed line in Fig. 3); this verifies the formation of the ZnS shell.

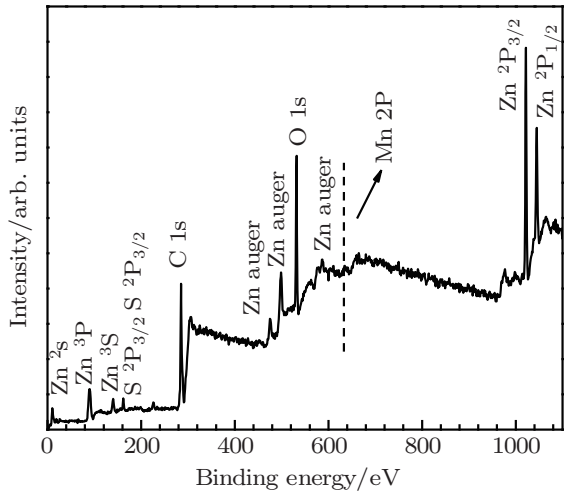


Fig. 3. XPS spectrum of MnS/ZnS core–shell QDs.

The PL excitation spectrum (monitored at 590 nm) and emission spectrum (excited by 325 nm) of the MnS/ZnS core–shell QDs are displayed in Figs. 4(a) and 4(b), respectively. The excitation spectrum has its maximum around 325 nm and shifts to the blue region of the spectrum compared with the excitation spectrum of the bulk ZnS. The excitation peaks from the d–d transition of Mn^{2+} ions are observed. Four absorption bands can be assigned to the transitions: $^6A_1$ (S) $\rightarrow$ ^4E (^4D), $^6A_1$ (S) $\rightarrow$ $^4T_2$ (^4D), $^6A_1$ (S) $\rightarrow$ $^4A_1$, ^4E (^4G), and $^6A_1$ (S) $\rightarrow$ $^4T_1$ (^4G).[20] Figure 4(b) shows the room-temperature PL spectrum of MnS/ZnS core–shell QDs at an excitation wavelength of 325 nm. There are two emission bands, one is a broad blue emission band around 448 nm and the other is an orange band at 590 nm. The blue emission band is associated with the trapped surface state[21,22] and the orange band is attributed to the transition $^4T_1 \rightarrow {}^6A_1$ of Mn^{2+} ions.[23,24] A schematic diagram of different emissions in the PL spectrum is illustrated in Fig. 5. Upon the excitation of 325 nm, electrons are excited into the conduction band of the ZnS host. Then the excited electrons can decay nonradiatively either to the ZnS surface states with emission in the blue region or to the Mn^{2+} 3d state leading to the orange emission.

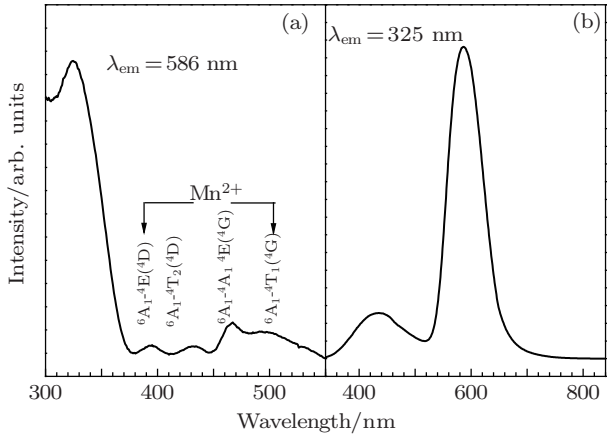


Fig. 4. PL excitation (a) and emission (b) spectra of MnS/ZnS core–shell QDs.

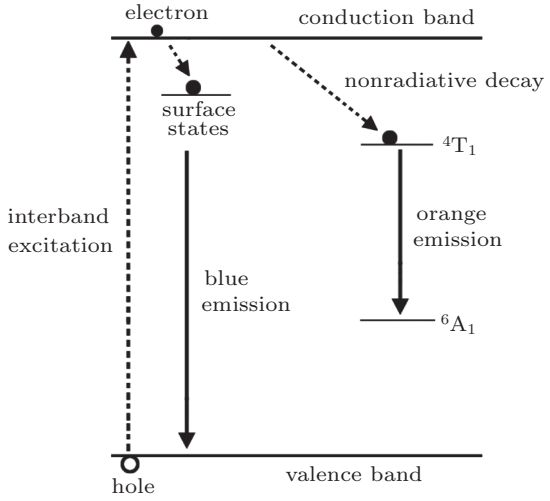


Fig. 5. Schematic diagram of the energy levels corresponding to different emissions in MnS/ZnS core–shell QDs.

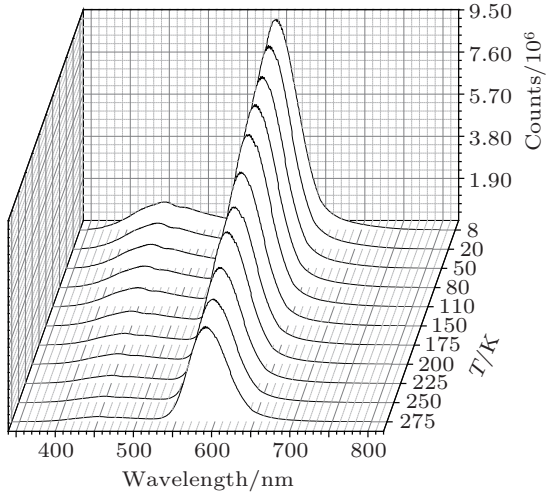


Fig. 6. PL spectra of MnS/ZnS core–shell QDs at different temperatures.

Figure 6 demonstrates the temperature-dependent PL spectra of MnS/ZnS core–shell QDs recorded in a temperature range of 8 K∼ 300 K. As the temperature increases, the orange emission shifts slightly towards the shorter wavelength. The blue shift of the orange emission with the increase of temperature is due to the reduction of the crystal field strength at higher temperatures as a result of crystal lattice expansion.[25] By increasing the temperature, the emitting state $^4T_1$ (G) of Mn^{2+} ions is lifted to a higher energy state and the orange emission thus shifts toward a shorter wavelength. On the contrary, the blue emission shifts toward a longer wavelength, which is consistent with the results obtained for ZnS:Mn QDs.[26] This is because the energy gap between the defects and the valence band increases as the temperature goes up due to crystal lattice expansion. The temperature dependences of the peak energies for both the orange emission and the blue emission are displayed in Fig. 7.

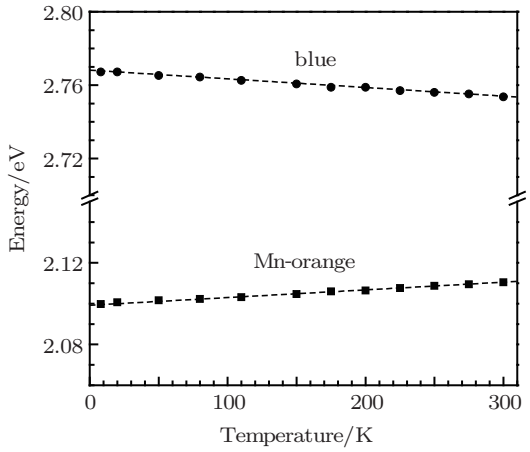


Fig. 7. Temperature dependences of peak energies for the blue and orange emissions in MnS/ZnS core–shell QDs.

It can be seen from Fig. 6 that all emissions from MnS/ZnS core–shell QDs decrease in intensity with an increase of temperature. The intensities are reduced respectively by approximately 52.3% for the orange emission and 85.7% for the blue emission with temperatures going from 8 K to 300 K. The blue emission then quenches faster than the orange emission as a function of temperature. Figure 8 shows the temperature-dependent variations of integrated intensity, i.e. the area under the peak, of the orange and blue emissions respectively. The temperature dependence of the intensity can be well described based on a thermal quenching theory as follows:[27]

$$I(T) = \frac{I_0}{1 + \sum_i a_i \exp(-E_i/k_B T)}, \quad (1)$$

where I_0 is the emission intensity at 0 K, a_i is a constant related to the ratio of the nonradiative rate to the radiative rate, k_B is the Boltzmann constant, and E_i is the activation energy (thermal quenching energy). According to the experimental data, there may be two thermal quenching processes responsible for the orange and blue emissions. One is a slow thermal

quenching process in a low temperature region and the other is a fast one in a high temperature region. Therefore, the variation of the luminescence intensity with temperature could be fitted using the following equation:

$$I(T) = \frac{I_0}{1 + a_1 \exp(-E_1/k_B T) + a_2 \exp(-E_2/k_B T)}. \quad (2)$$

Each of the solid lines in Fig. 8 represents a fitting result to the experimental data by using Eq. (2) with those fitting parameters listed in Table 1. This fact indicates that the luminescence intensities for the two emissions are lowered indeed, owing to thermal quenching. For the orange and blue emissions the optical 325-nm excitation is the indirect excitation. This means that there are two thermal quenching channels for the orange and blue emissions respectively. The rapid decrease in intensity at high temperatures can be attributed to the thermally activated nonradiative mechanism with strong temperature dependence, and the slow decrease in intensity may be due to other nonradiative recombination mechanisms with weak temperature dependence.

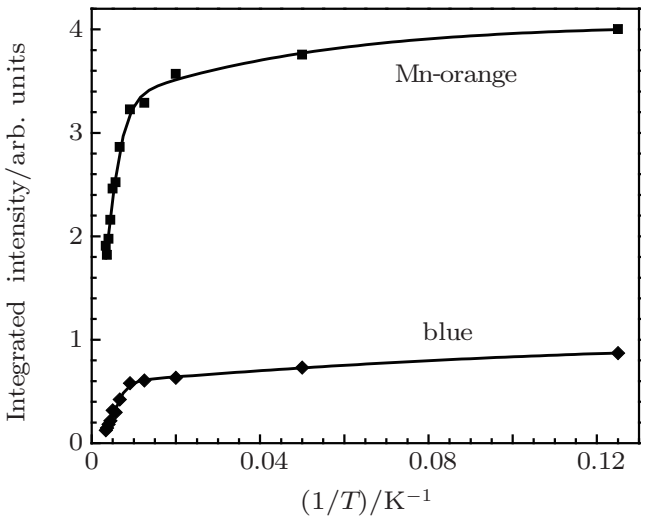


Fig. 8. Temperature dependences of integrated intensity for the blue and orange emission in MnS/ZnS core–shell QDs respectively. The solid lines represent the fitting results using Eq. (2).

Table 1. Fitting parameters for the temperature dependences of orange and blue emissions in MnS/ZnS core–shell QDs.

	a_1	a_2	E_1/meV	E_2/meV
Orange emission	0.25±0.06	4.74±0.15	2.10±0.57	39.36±0.84
Blue emission	0.69±0.22	51.24±9.12	1.23±0.07	56.32±0.14

For the orange emission, the large activation energy of E_2 is likely to be due to the thermal dissociation of excitons in the ZnS host while the small activation energy of E_1 may be associated with the desorption of excitons from the Mn^{2+} ions. The activation energy of 56.32 meV for the blue emission is larger than 39.36 meV for the orange emission. Because the thermal activation energy is related to the bound exciton binding energy, the larger activation energy indicates that exciton binding energy is strongly related to the defect state centers as compared with the Mn^{2+} ions. Furthermore, the value of a for the blue emission is larger than for the orange emission, indicating that the nonradiative rate is greater for the blue emission than for the orange emission. It is generally believed that the major nonradiative or energy relaxation channel in a semiconductor is phonon quenching.[28] If the phonon coupling is stronger, the nonradiative rate is higher and the luminescence is more sensitive to temperature.[27] The fitting results show that the phonon coupling for the defect centers is stronger than that for the Mn^{2+} ions. This is in agreement with the fact that the luminescence of the blue emission quenches faster than that of the orange emission as a function of temperature.

4. Conclusion

In this paper, the temperature dependence of the PL for MnS/ZnS core–shell QDs is investigated in a temperature range between 8 K and 300 K. The orange emission is assigned to the $^4T_1 \rightarrow {}^6A_1$ transition of Mn^{2+} ions, and the blue emission is assigned to the emission of the trapped surface state of ZnS. As the temperature increases from 8 K to 300 K, the orange emission shifts towards a shorter wavelength while the blue emission shifts towards a longer wavelength. The luminescence intensities of the orange and blue emissions decrease with the increase of temperature but the blue emission quenches faster than the orange emission. The temperature dependences of the two emissions can be explained well by the thermal quenching theory.

References

[1] Zheng S W, He M, Li S T and Zhang Y 2014 *Chin. Phys. B* **23** 087101
[2] Xia Y J, Guang Z S and He T 2014 *Chin. Phys. B* **23** 087701
[3] Tan Y and Wang Y G 2013 *Chin. Phys. Lett.* **30** 117901
[4] Chandra V K, Chandra B P and Jha P 2013 *Appl. Phys. Lett.* **103** 161113
[5] Fang X S, Bando Y, Liao M Y, Gautam U K, Zhi C Y, Dierre B, Liu B D, Zhai T Y, Sekiguchi T, Koide Y and Golberg D 2009 *Adv. Mater.* **21** 2034
[6] Ma L, Jiang K, Liu X T and Chen W 2014 *J. Appl. Phys.* **115** 103104
[7] He E J, Zheng H R, Gao W, Lu Y, Li J N, Wei Y, Wang D and Zhu G Q 2013 *Acta Phys. Sin.* **62** 237803 (in Chinese)
[8] Wood V, Halpert J E, Panzer M J, Bawendi M G and Bulovic V 2009 *Nano Lett.* **9** 2367
[9] Alivisatos A P 1996 *J. Phys. Chem.* **100** 13226
[10] Yang H and Holloway P H 2004 *Adv. Funct. Mater.* **14** 152
[11] Yang H, Holloway P H, Cunningham G and Schanze K S 2004 *J. Chem. Phys.* **121** 10233
[12] Karar N, Chander H and Shivaprasad S M 2004 *Appl. Phys. Lett.* **85** 5058
[13] Hattori Y, Isobe T, Takahashi H and Itoh S 2005 *J. Lumin.* **113** 69
[14] Jiang D X, Cao L X, Su G, Qu H and Sun D K 2007 *Appl. Surf. Sci.* **253** 9330

[15] Quan Z W, Wang Z L, Yang P P, Lin J and Fang J Y 2007 *Inorg. Chem.* **46** 1354
[16] Xie D N, Peng H S, Huang S H, You F T and Wang X H 2014 *Acta Phys. Sin.* **63** 147801 (in Chinese)
[17] Zheng J J, Yuan X, Ikezawa M, Jing P T, Liu X Y, Zheng Z H, Kong X G, Zhao J L and Masumoto Y 2009 *J. Phys. Chem. C* **113** 16969
[18] Zheng J J, Ji W Y, Wang X Y, Ikezawa M, Jing P T, Liu X Y, Li H B, Zhao J L and Masumoto Y 2010 *J. Phys. Chem. C* **114** 15331
[19] Dai R C, Zheng J J, Zhang C C, Zhang Z M and Ding Z J 2011 *J. Nanosci. Nanotechnol.* **11** 9883
[20] Peng W Q, Qu S C, Cong G W, Zhang X Q and Wang Z G 2005 *J. Cryst. Growth* **282** 179
[21] Bol A A and Meijerink A 1998 *Phys. Rev. B* **58** R15997
[22] Sharma M, Singh S and Pandey O P 2010 *J. Appl. Phys.* **107** 104319
[23] Bhargava R N, Gallagher D, Hong X and Nurmikko A 1994 *Phys. Rev. Lett.* **72** 416
[24] Murase N, Jagannathan R, Kanematsu Y, Watanabe M, Kurita A, Hirata K, Yazawa T and Kushida T 1999 *J. Phys. Chem. B* **103** 754
[25] Joly A G, Chen W, Roark J and Zhang J Z 2001 *J. Nanosci. Nanotechnol.* **1** 295
[26] Su F H, Ma B S, Fang Z L, Ding K, Li G H and Chen W 2002 *J. Phys.: Condens. Mater* **14** 12657
[27] Leroux M, Grandjean N, Beaumont B, Nataf G, Semond F, Massies J and Gibart P 1999 *J. Appl. Phys.* **86** 3721
[28] Huang K and Rhys A 1950 *Proc. R. Soc. London A* **204** 406